

Observation of $B \rightarrow \phi\phi K$

H.-C. Huang,²⁵ K. Abe,⁷ K. Abe,⁴⁰ T. Abe,⁴¹ I. Adachi,⁷ H. Aihara,⁴² M. Akatsu,²¹ T. Aso,⁴⁶ V. Aulchenko,² T. Aushev,¹¹ A. M. Bakich,³⁷ Y. Ban,³² E. Banas,²⁶ A. Bay,¹⁷ I. Bedny,² P. K. Behera,⁴⁷ I. Bizjak,¹² A. Bondar,² A. Bozek,²⁶ M. Bračko,^{19,12} T. E. Browder,⁶ B. C. K. Casey,⁶ P. Chang,²⁵ Y. Chao,²⁵ K.-F. Chen,²⁵ B. G. Cheon,³⁶ R. Chistov,¹¹ Y. Choi,³⁶ Y. K. Choi,³⁶ M. Danilov,¹¹ L. Y. Dong,⁹ A. Drutskoy,¹¹ S. Eidelman,² V. Eiges,¹¹ Y. Enari,²¹ C. Fukunaga,⁴⁴ N. Gabyshev,⁷ A. Garmash,^{2,7} T. Gershon,⁷ B. Golob,^{18,12} R. Guo,²³ J. Haba,⁷ F. Handa,⁴¹ T. Hara,³⁰ N. C. Hastings,⁷ H. Hayashii,²² M. Hazumi,⁷ L. Hinz,¹⁷ T. Hokuue,²¹ Y. Hoshi,⁴⁰ W.-S. Hou,²⁵ Y. B. Hsiung,^{25,*} Y. Igarashi,⁷ T. Iijima,²¹ K. Inami,²¹ A. Ishikawa,²¹ R. Itoh,⁷ Y. Iwasaki,⁷ H. K. Jang,³⁵ J. H. Kang,⁵⁰ J. S. Kang,¹⁴ P. Kapusta,²⁶ N. Katayama,⁷ H. Kawai,³ N. Kawamura,¹ T. Kawasaki,²⁸ H. Kichimi,⁷ D. W. Kim,³⁶ H. J. Kim,⁵⁰ Hyunwoo Kim,¹⁴ J. H. Kim,³⁶ K. Kinoshita,⁵ P. Koppenburg,⁷ S. Korpar,^{19,12} P. Krizán,^{18,12} P. Krokovny,² R. Kulasiri,⁵ S. Kumar,³¹ Y.-J. Kwon,⁵⁰ G. Leder,¹⁰ S. H. Lee,³⁵ T. Lesiak,²⁶ J. Li,³⁴ A. Limosani,²⁰ S.-W. Lin,²⁵ D. Liventsev,¹¹ J. MacNaughton,¹⁰ G. Majumder,³⁸ F. Mandl,¹⁰ D. Marlow,³³ H. Matsumoto,²⁸ T. Matsumoto,⁴⁴ W. Mitaroff,¹⁰ H. Miyata,²⁸ G. R. Moloney,²⁰ T. Mori,⁴ T. Nagamine,⁴¹ Y. Nagasaka,⁸ T. Nakadaira,⁴² E. Nakano,²⁹ M. Nakao,⁷ H. Nakazawa,⁷ J. W. Nam,³⁶ Z. Natkaniec,²⁶ S. Nishida,¹⁵ O. Nitoh,⁴⁵ T. Nozaki,⁷ S. Ogawa,³⁹ T. Ohshima,²¹ T. Okabe,²¹ S. Okuno,¹³ S. L. Olsen,⁶ W. Ostrowicz,²⁶ H. Ozaki,⁷ H. Palka,²⁶ C. W. Park,¹⁴ H. Park,¹⁶ K. S. Park,³⁶ N. Parslow,³⁷ J.-P. Perroud,¹⁷ M. Peters,⁶ L. E. Piilonen,⁴⁸ M. Rozanska,²⁶ H. Sagawa,⁷ S. Saitoh,⁷ Y. Sakai,⁷ T. R. Sarangi,⁴⁷ A. Satpathy,^{7,5} O. Schneider,¹⁷ J. Schümann,²⁵ C. Schwanda,^{7,10} A. J. Schwartz,⁵ T. Seki,⁴⁴ S. Semenov,¹¹ M. E. Sevier,²⁰ T. Shibata,²⁸ H. Shibuya,³⁹ V. Sidorov,² J. B. Singh,³¹ S. Stanić,^{7,†} M. Starić,¹² A. Sugi,²¹ K. Sumisawa,⁷ T. Sumiyoshi,⁴⁴ S. Suzuki,⁴⁹ S. Y. Suzuki,⁷ T. Takahashi,²⁹ F. Takasaki,⁷ K. Tamai,⁷ N. Tamura,²⁸ J. Tanaka,⁴² M. Tanaka,⁷ G. N. Taylor,²⁰ Y. Teramoto,²⁹ T. Tomura,⁴² S. N. Tovey,²⁰ K. Trabelsi,⁶ T. Tsuboyama,⁷ T. Tsukamoto,⁷ S. Uehara,⁷ S. Uno,⁷ G. Varner,⁶ K. E. Varvell,³⁷ C. C. Wang,²⁵ C. H. Wang,²⁴ J. G. Wang,⁴⁸ M.-Z. Wang,²⁵ Y. Watanabe,⁴³ E. Won,¹⁴ B. D. Yabsley,⁴⁸ Y. Yamada,⁷ A. Yamaguchi,⁴¹ Y. Yamashita,²⁷ M. Yamauchi,⁷ H. Yanai,²⁸ Heyoung Yang,³⁵ Y. Yusa,⁴¹ C. C. Zhang,⁹ Z. P. Zhang,³⁴ Y. Zheng,⁶ V. Zhilich,² and D. Žontar^{18,12}

(Belle Collaboration)

¹Aomori University, Aomori

²Budker Institute of Nuclear Physics, Novosibirsk

³Chiba University, Chiba

⁴Chuo University, Tokyo

⁵University of Cincinnati, Cincinnati, Ohio 45221

⁶University of Hawaii, Honolulu, Hawaii 96822

⁷High Energy Accelerator Research Organization (KEK), Tsukuba

⁸Hiroshima Institute of Technology, Hiroshima

⁹Institute of High Energy Physics, Chinese Academy of Sciences, Beijing

¹⁰Institute of High Energy Physics, Vienna

¹¹Institute for Theoretical and Experimental Physics, Moscow

¹²J. Stefan Institute, Ljubljana

¹³Kanagawa University, Yokohama

¹⁴Korea University, Seoul

¹⁵Kyoto University, Kyoto

¹⁶Kyungpook National University, Taegu

¹⁷Institut de Physique des Hautes Énergies, Université de Lausanne, Lausanne

¹⁸University of Ljubljana, Ljubljana

¹⁹University of Maribor, Maribor

²⁰University of Melbourne, Victoria

²¹Nagoya University, Nagoya

²²Nara Women's University, Nara

²³National Kaohsiung Normal University, Kaohsiung

²⁴National Lien-Ho Institute of Technology, Miao Li

²⁵Department of Physics, National Taiwan University, Taipei

²⁶H. Niewodniczanski Institute of Nuclear Physics, Krakow

²⁷Nihon Dental College, Niigata

²⁸Niigata University, Niigata

²⁹Osaka City University, Osaka

³⁰Osaka University, Osaka

³¹*Panjab University, Chandigarh*³²*Peking University, Beijing*³³*Princeton University, Princeton, New Jersey 08545*³⁴*University of Science and Technology of China, Hefei*³⁵*Seoul National University, Seoul*³⁶*Sungkyunkwan University, Suwon*³⁷*University of Sydney, Sydney NSW*³⁸*Tata Institute of Fundamental Research, Bombay*³⁹*Toho University, Funabashi*⁴⁰*Tohoku Gakuin University, Tagajo*⁴¹*Tohoku University, Sendai*⁴²*Department of Physics, University of Tokyo, Tokyo*⁴³*Tokyo Institute of Technology, Tokyo*⁴⁴*Tokyo Metropolitan University, Tokyo*⁴⁵*Tokyo University of Agriculture and Technology, Tokyo*⁴⁶*Toyama National College of Maritime Technology, Toyama*⁴⁷*Utkal University, Bhubaneswar*⁴⁸*Virginia Polytechnic Institute and State University, Blacksburg, Virginia 24061*⁴⁹*Yokkaichi University, Yokkaichi*⁵⁰*Yonsei University, Seoul*

We report the observation of the decay mode $B \rightarrow \phi\phi K$ based on an analysis of 78 fb^{-1} of data collected with the Belle detector at KEKB. This is the first example of a $b \rightarrow s\bar{s}s\bar{s}$ transition. The branching fraction for this decay is measured to be $\mathcal{B}(B^\pm \rightarrow \phi\phi K^\pm) = (2.6_{-0.9}^{+1.1} \pm 0.3) \times 10^{-6}$ for a $\phi\phi$ invariant mass below $2.85 \text{ GeV}/c^2$. Results for other related charmonium decay modes are also reported.

PACS numbers: 13.25.Hw, 14.40.Nd

We report the observation of the decay mode $B \rightarrow \phi\phi K$, the first example of a $b \rightarrow s\bar{s}s\bar{s}$ transition. In the Standard Model (SM), this decay channel requires the creation of an additional final $s\bar{s}$ quark pair than in $b \rightarrow s\bar{s}$ processes, which have been previously observed in modes such as $B \rightarrow \phi K$. In addition to improving our understanding of charmless B decays, the $\phi\phi K$ state may be sensitive to glueball production in B decays, where the glueball decays to $\phi\phi$ [1]. In addition, with sufficient statistics, the decay $B \rightarrow \phi\phi K$ could be used to search for a possible non-SM CP -violating phase in the $b \rightarrow s$ transition [2]. Direct CP violation could be enhanced to as high as the 40% level if there is sizable interference between transitions due to non-SM physics and decays via the η_c resonance.

We use a 78 fb^{-1} data sample collected with the Belle detector at the KEKB asymmetric-energy e^+e^- (3.5 on 8 GeV) collider [3] operating at the $\Upsilon(4S)$ resonance ($\sqrt{s} = 10.58 \text{ GeV}$). The sample contains 85.0×10^6 produced $B\bar{B}$ pairs. The Belle detector is a large-solid-angle magnetic spectrometer consisting of a three-layer silicon vertex detector, a 50-layer central drift chamber (CDC), a system of aerogel threshold Čerenkov counters (ACC), time-of-flight scintillation counters (TOF), and an array of CsI(Tl) crystals located inside a superconducting solenoid coil that provides a 1.5 T magnetic field. An iron flux-return located outside of the coil is instrumented to identify K_L^0 and muons. The detector is described in detail elsewhere [4].

We select well measured charged tracks that have im-

pact parameters with respect to the nominal interaction point (IP) that are less than 0.2 cm in the radial direction and less than 2 cm along the beam direction (z). Each track is identified as a kaon or a pion according to a K/π likelihood ratio, $\mathcal{L}_K/(\mathcal{L}_\pi + \mathcal{L}_K)$, where $\mathcal{L}_{K(\pi)}$ are likelihoods derived from responses of the TOF and ACC systems and dE/dx measurements in the CDC. We select kaon candidates by requiring $\mathcal{L}_K/(\mathcal{L}_\pi + \mathcal{L}_K) > 0.6$. This requirement is 88% efficient for kaons with a 8.5% misidentification rate for pions. Kaon candidates that are electron-like according to the information recorded in the CsI(Tl) calorimeter are rejected.

Candidate ϕ mesons are reconstructed via the $\phi \rightarrow K^+K^-$ decay mode; we require the K^+K^- invariant mass to be within $\pm 20 \text{ MeV}/c^2$ (± 4.5 times the full width) of the ϕ mass [5]. For the $B^0(\bar{B}^0) \rightarrow \phi\phi K_S^0$ decay mode, we use $K_S^0 \rightarrow \pi^+\pi^-$ candidates in the mass window $482 \text{ MeV}/c^2 < M(\pi^+\pi^-) < 514 \text{ MeV}/c^2$ ($\pm 4\sigma$), where the distance of closest approach between the two daughter tracks is less than 2.4 cm , the magnitude of the impact parameter of each track in the radial direction exceeds 0.02 cm , and the flight length is greater than 0.22 cm . The difference in the angle between the pion-pair vertex direction from the IP and its reconstructed flight direction in the $x-y$ plane is required to be less than 0.03 radians.

To isolate the signal, we form the beam-constrained mass, $M_{bc} = \sqrt{E_{\text{beam}}^2 - |\vec{P}_{\text{recon}}|^2}$, and the energy difference $\Delta E = E_{\text{recon}} - E_{\text{beam}}$. Here E_{beam} is the

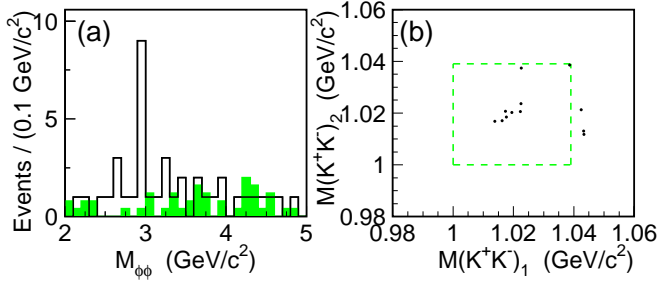


FIG. 1: (a) $\phi\phi$ invariant mass spectrum. The open histogram corresponds to events from the $B^\pm \rightarrow \phi\phi K^\pm$ signal region and the shaded histogram corresponds to events from the M_{bc} - ΔE sidebands. (b) $M_{K^+K^-}$ of one ϕ meson candidate versus $M_{K^+K^-}$ of the other for the events satisfying $M_{\phi\phi} < 2.85$ GeV/c^2 . The events are concentrated near the point (M_ϕ, M_ϕ) . The dashed box shows the region selected for the $B \rightarrow \phi\phi K$ analysis.

beam energy, and E_{recon} and \vec{P}_{recon} are the reconstructed energy and momentum of the signal candidate in the $\Upsilon(4S)$ center-of-mass frame. The signal region for ΔE is ± 30 MeV which corresponds to $\pm 3.1\sigma$, where σ is the resolution determined from a Gaussian fit to the Monte Carlo (MC) simulation. The signal region for M_{bc} is $5.27 \text{ GeV}/c^2 < M_{bc} < 5.29 \text{ GeV}/c^2$. The beam-constrained mass resolution is $2.8 \text{ MeV}/c^2$, which is mostly due to the beam energy spread of KEKB.

The major background for the $B \rightarrow \phi\phi K$ process is from continuum $e^+e^- \rightarrow q\bar{q}$ production, where q is a light quark (u, d, s , or c). Several event topology variables are used to discriminate the continuum background, which tends to be collimated along the original quark direction, from the more isotropic $B\bar{B}$ events. Five modified Fox-Wolfram moments, the S_\perp variable [6] and the cosine of the thrust angle are combined into a Fisher discriminant [7]. We form signal and background probability density functions (PDFs) for this Fisher discriminant and for the cosine of the B decay angle with respect to the z axis ($\cos\theta_B$) for the signal MC and sideband ($5.20 \text{ GeV}/c^2 < M_{bc} < 5.26 \text{ GeV}/c^2$ and $0.1 < |\Delta E| < 0.2$ GeV) data, respectively. The PDFs are multiplied together to form signal and background likelihoods, \mathcal{L}_S and \mathcal{L}_{BG} . The likelihood ratio $\mathcal{LR} \equiv \mathcal{L}_S/(\mathcal{L}_S + \mathcal{L}_{BG})$ is then required to be greater than 0.1. This requirement retains 97% of the signal while removing 55% of the continuum background.

Figure 1(a) shows the $\phi\phi$ invariant mass spectrum for events in the $B^\pm \rightarrow \phi\phi K^\pm$ signal region, where a clear η_c peak and some excess in the lower mass region are evident.

To extract signal yields, we apply an unbinned, extended maximum likelihood (ML) fit to the events with $|\Delta E| < 0.2$ GeV and $M_{bc} > 5.2$ GeV/c^2 . The extended likelihood for a sample of N events is $\mathcal{L} = e^{-(N_S + N_B)} \prod_{i=1}^N (N_S \mathcal{P}_i^S + N_B \mathcal{P}_i^B)$, where $\mathcal{P}_i^{S(B)}$ describes

the probability for candidate event i to belong to the signal (background), based on its measured M_{bc} and ΔE values. The exponential factor in the likelihood accounts for Poisson fluctuations in the total number of observed events N . The signal yield N_S and the number of background events N_B are obtained by maximizing \mathcal{L} . The statistical errors correspond to unit changes in the quantity $\chi^2 = -2\ln\mathcal{L}$ around its minimum value. The significance of the signal is defined as the square root of the change in χ^2 when constraining the number of signal events to zero in the likelihood fit; it reflects the probability for the background to fluctuate to the observed event yield.

The probability \mathcal{P} for a given event i is calculated as the product of independent PDFs for M_{bc} and ΔE . The signal PDFs are represented by a Gaussian for M_{bc} and a double Gaussian for ΔE . The background PDF for ΔE is a linear function; for the M_{bc} background we use a phase-space-like function with an empirical shape [8]. The parameters of the PDFs are determined from high-statistics MC samples for the signal and sideband data for the background.

For $M(\phi\phi) < 2.85 \text{ GeV}/c^2$, the region below the charm threshold, the ML fit gives an event yield of $7.3^{+3.2}_{-2.5}$ with a significance of 5.1 standard deviations (σ). Projections of the ΔE distribution (with $5.27 \text{ GeV}/c^2 < M_{bc} < 5.29 \text{ GeV}/c^2$) and of the M_{bc} distribution (with $|\Delta E| < 30$ MeV) are shown in Figs. 2(a,b). As a consistency check, a ML fit to the projected ΔE distribution (Fig. 2(b) only gives a signal yield of $7.5^{+3.3}_{-2.7}$ with a 4.8σ statistical significance. Figure 1(b) shows a scatter plot of the two K^+K^- invariant masses for events in the B meson signal region with $M(K^+K^-K^+K^-) < 2.85 \text{ GeV}/c^2$ with the ϕ mass requirements relaxed. Here there is a clear concentration in the overlap region of the two ϕ bands. There is no event excess in the ϕ mass sidebands, which leads us to conclude that the observed signal is entirely due to $B^\pm \rightarrow \phi\phi K^\pm$. Using a signal efficiency of 3.3%, obtained from a large-statistics MC that uses three-body phase space to model the $B^\pm \rightarrow \phi\phi K^\pm$ decays, we determine the branching fraction for charmless $B^\pm \rightarrow \phi\phi K^\pm$ with $M_{\phi\phi} < 2.85 \text{ GeV}/c^2$ to be

$$\mathcal{B}(B^\pm \rightarrow \phi\phi K^\pm) = (2.6^{+1.1}_{-0.9} \pm 0.3) \times 10^{-6},$$

where the first error is statistical and the second is systematic.

Contributions to the systematic error include the uncertainties due to the tracking efficiency (5.4%), particle identification efficiency (5%), and the modeling of the likelihood ratio cut (2%). The error due to the modeling of the likelihood ratio cut is determined using $B^- \rightarrow D^0(\rightarrow K^-\pi^+\pi^-\pi^+)\pi^-$ events in the same data sample; these events have the same number of final-state particles and an event topology that is similar to the $B^\pm \rightarrow \phi\phi K^\pm$ signal. The uncertainty due to the MC $M_{\phi\phi}$ modeling (4%) accounts for the $M_{\phi\phi}$ dependence of

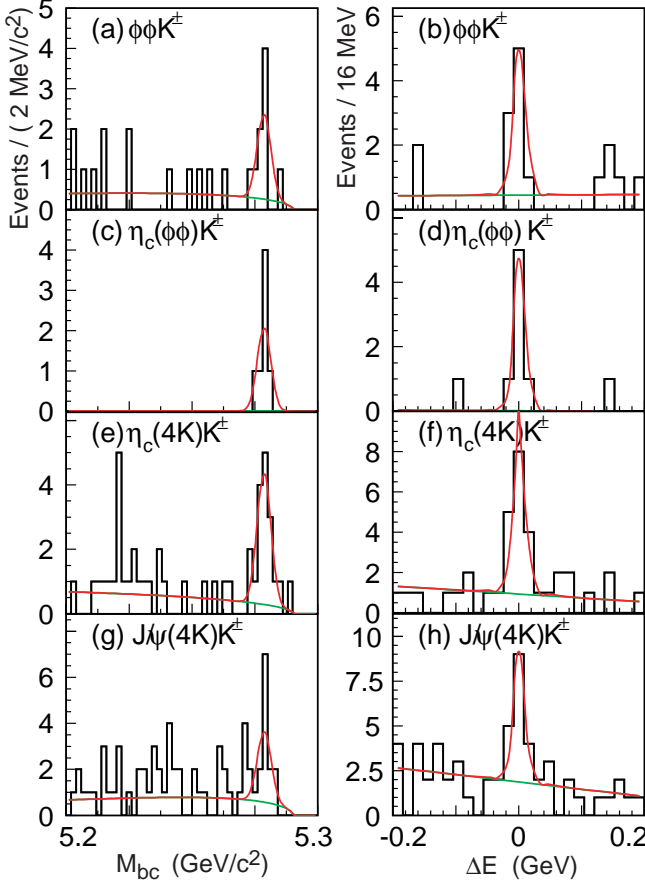


FIG. 2: Projections of M_{bc} and ΔE overlaid with the fitted curves for (a, b) $B^\pm \rightarrow \phi\phi K^\pm$ with $M_{\phi\phi} < 2.85 \text{ GeV}/c^2$, (c, d) $B^\pm \rightarrow \eta_c K^\pm$ and $\eta_c \rightarrow \phi\phi$, (e, f) $B^\pm \rightarrow \eta_c(4K)K^\pm$ and $\eta_c \rightarrow 2(K^+K^-)$, and (g, h) $B^\pm \rightarrow J/\psi(4K)K^\pm$ and $J/\psi \rightarrow 2(K^+K^-)$.

the detection efficiency. The systematic error in the signal yield (6%) is determined by varying the means and σ of the signal and the shape parameters of the background. We determine an upper limit of 5% on the possible contamination by non-resonant $B^\pm \rightarrow \phi(K^+K^-)_{\text{NR}}K^\pm$ or $B^\pm \rightarrow 2(K^+K^-)_{\text{NR}}K^\pm$ decays by redoing the fits with the ϕ mass requirement relaxed. The sources of systematic error are combined in quadrature to obtain the final systematic error of 12%.

For the $B^0(\bar{B}^0) \rightarrow \phi\phi K_S^0$ mode, there are only four signal candidates. We combine the $B^\pm \rightarrow \phi\phi K^\pm$ and $B^0(\bar{B}^0) \rightarrow \phi\phi K_S^0$ modes and perform a ML fit and obtain a signal event yield of $8.7^{+3.6}_{-2.9}$ with 5.3σ statistical significance. Assuming isospin symmetry, we obtain

$$\mathcal{B}(B \rightarrow \phi\phi K) = (2.3^{+0.9}_{-0.8} \pm 0.3) \times 10^{-6},$$

for $M_{\phi\phi} < 2.85 \text{ GeV}/c^2$.

No enhancement is observed in the $M_{\phi\phi}$ region corresponding to the $f_J(2220)$ glueball candidate [5], also referred to as ξ . Assuming the mass and width of $f_J(2220)$ to be $2230 \text{ MeV}/c^2$ and $20 \text{ MeV}/c^2$, we define a signal region

of $2.19 \text{ GeV}/c^2 < M_{\phi\phi} < 2.27 \text{ GeV}/c^2$, $5.27 \text{ GeV}/c^2 < M_{bc} < 5.29 \text{ GeV}/c^2$ and $|\Delta E| < 30 \text{ MeV}$. One event is observed in this region with an expected background, estimated from the sideband, of 0.5. Using an extended Cousins-Highland method that uses the the Feldman-Cousins ordering scheme and takes systematic uncertainties into account [9], we obtain a 90% confidence level (CL) upper limit of 3.7 signal events, which corresponds to

$$\mathcal{B}(B^\pm \rightarrow f_J(2220)K^\pm) \times \mathcal{B}(f_J(2220) \rightarrow \phi\phi) < 1.2 \times 10^{-6}.$$

We select $B^\pm \rightarrow \eta_c K^\pm$, $\eta_c \rightarrow \phi\phi$ candidates by requiring $2.94 \text{ GeV}/c^2 < M_{\phi\phi} < 3.02 \text{ GeV}/c^2$. A clear signal is evident in Figures 2(c,d), and the fitted yield of $N_S = 7.0^{+3.0}_{-2.3}$ events has a significance of 8.8σ . The corresponding branching fraction is

$$\begin{aligned} \mathcal{B}(B^\pm \rightarrow \eta_c K^\pm) \times \mathcal{B}(\eta_c \rightarrow \phi\phi) \\ = (2.2^{+1.0}_{-0.7} \pm 0.5) \times 10^{-6}. \end{aligned}$$

In addition to the previously listed sources of systematic error, here the error also includes the possible contamination from charmless $B^\pm \rightarrow \phi\phi K^\pm$ decays, which is estimated to be less than 1.2 events. Using the measured branching fraction $\mathcal{B}(B^\pm \rightarrow \eta_c K^\pm) = (1.25 \pm 0.42) \times 10^{-3}$ [10], we determine the $\eta_c \rightarrow \phi\phi$ branching fraction to be

$$\mathcal{B}(\eta_c \rightarrow \phi\phi) = (1.8^{+0.8}_{-0.6} \pm 0.7) \times 10^{-3},$$

which is smaller than the current world average value of $(7.1 \pm 2.8) \times 10^{-3}$ [5].

Since the J/ψ and η_c charmonium resonances also decay to $2(K^+K^-)$, the decay chains $B \rightarrow \text{charmonium} + K$ with charmonium $\rightarrow 2(K^+K^-)$ can provide consistency checks of the $B \rightarrow \phi\phi K$ analysis. To select $B \rightarrow 2(K^+K^-)K$ candidates, we apply tighter particle identification and continuum suppression requirements than in the case of $B \rightarrow \phi\phi K$ in order to reduce the larger combinatoric background. Figure 3(a) shows the invariant mass distribution of any two pairs of K^+K^- , M_{4K} , between $2.8 \text{ GeV}/c^2$ and $3.2 \text{ GeV}/c^2$ for the events in the B signal region. Significant contributions from both η_c and J/ψ intermediate states are seen.

To identify the signals from η_c and J/ψ intermediate states, we require that the invariant mass of $2(K^+K^-)$ satisfy $2.94 \text{ GeV}/c^2 < M_{4K} < 3.02 \text{ GeV}/c^2$ and $3.06 \text{ GeV}/c^2 < M_{4K} < 3.14 \text{ GeV}/c^2$, respectively. We use signal yields from ML fits to determine branching fractions. Figures 2(e-h) show the M_{bc} and ΔE projection plots with the fitted curves superimposed. Table I summarizes the signal yields, efficiencies, statistical significances, and the branching-fraction products. By requiring the invariant mass of one of the K^+K^- pairs to correspond to a ϕ meson, we also measure the decays of $B^\pm \rightarrow \eta_c(J/\psi)K^\pm$ and $\eta_c(J/\psi) \rightarrow \phi K^+K^-$. The results are included in Table I.

TABLE I: Signal yields, efficiencies including secondary branching fractions, statistical significances and branching fractions of $B \rightarrow \phi\phi K$ and related decays. The branching fractions for modes with K^+K^- pairs include contributions from $\phi \rightarrow K^+K^-$.

Mode	Yield	Efficiency (%)	Significance (σ)	$\mathcal{B} (\times 10^{-6})$
$B^\pm \rightarrow \phi\phi K^\pm$ ($M_{\phi\phi} < 2.85 \text{ GeV}/c^2$)	$7.3^{+3.2}_{-2.5}$	3.3	5.1	$2.6^{+1.1}_{-0.9} \pm 0.3$
$B \rightarrow \phi\phi K$ ($M_{\phi\phi} < 2.85 \text{ GeV}/c^2$)	$8.7^{+3.6}_{-2.9}$	2.2	5.3	$2.3^{+0.9}_{-0.8} \pm 0.3$
$B^\pm \rightarrow f_J(2220)K^\pm, f_J(2220) \rightarrow \phi\phi$	< 3.7	3.6	.	< 1.2
$B^\pm \rightarrow \eta_c K^\pm, \eta_c \rightarrow \phi\phi$	$7.0^{+3.0}_{-2.3}$	3.7	8.8	$2.2^{+1.0}_{-0.7} \pm 0.5$
$B^\pm \rightarrow \eta_c K^\pm, \eta_c \rightarrow \phi K^+ K^-$	$14.1^{+4.4}_{-3.7}$	4.6	7.7	$3.6^{+1.1}_{-0.8} \pm 0.8$
$B^\pm \rightarrow \eta_c K^\pm, \eta_c \rightarrow 2(K^+ K^-)$	$14.6^{+4.6}_{-3.9}$	9.6	6.6	$1.8^{+0.9}_{-0.5} \pm 0.4$
$B^\pm \rightarrow J/\psi K^\pm, J/\psi \rightarrow \phi K^+ K^-$	$9.0^{+3.7}_{-3.0}$	4.4	5.3	$2.4^{+1.0}_{-0.8} \pm 0.3$
$B^\pm \rightarrow J/\psi K^\pm, J/\psi \rightarrow 2(K^+ K^-)$	$11.0^{+4.3}_{-3.5}$	9.2	4.8	$1.4^{+0.6}_{-0.4} \pm 0.2$

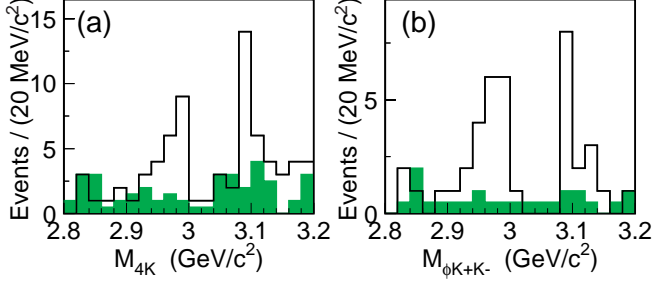


FIG. 3: (a) $2(K^+K^-)$ and (b) $\phi K^+ K^-$ invariant mass spectra in the η_c and J/ψ regions. The open histograms correspond to events from the B signal region, and the shaded histograms correspond to events from the $M_{bc}-\Delta E$ sidebands.

TABLE II: Measured branching fractions of secondary charmonium decays and the world averages [5]. The branching fractions for modes with K^+K^- pairs include contributions from $\phi \rightarrow K^+K^-$.

Decay mode	\mathcal{B} (this work)	\mathcal{B} (PDG)
$\eta_c \rightarrow \phi\phi$	$(1.8^{+0.8}_{-0.6} \pm 0.7) \times 10^{-3}$	$(7.1 \pm 2.8) \times 10^{-3}$
$\eta_c \rightarrow \phi K^+ K^-$	$(2.9^{+0.9}_{-0.8} \pm 1.1) \times 10^{-3}$	—
$\eta_c \rightarrow 2(K^+ K^-)$	$(1.4^{+0.5}_{-0.4} \pm 0.6) \times 10^{-3}$	$(2.1 \pm 1.2) \%$
$J/\psi \rightarrow \phi K^+ K^-$	$(2.4^{+1.0}_{-0.8} \pm 0.3) \times 10^{-3}$	$(7.4 \pm 1.1) \times 10^{-4}$
$J/\psi \rightarrow 2(K^+ K^-)$	$(1.4^{+0.5}_{-0.4} \pm 0.2) \times 10^{-3}$	$(7.0 \pm 3.0) \times 10^{-4}$

Using the known branching fractions $\mathcal{B}(B^\pm \rightarrow J/\psi K^\pm) = (1.01 \pm 0.05) \times 10^{-3}$ [5] and $\mathcal{B}(B^\pm \rightarrow \eta_c K^\pm)$, we obtain the secondary branching fractions for J/ψ and η_c decays to $2(K^+K^-)$ and $\phi K^+ K^-$ listed in Table II.

Our measured branching fractions for $\eta_c \rightarrow \phi\phi$ and $\eta_c \rightarrow 2(K^+K^-)$ are smaller than those of previous experiments [5], while those for J/ψ decays are consistent. The decay $\eta_c \rightarrow 2(K^+K^-)$ proceeds dominantly through $\eta_c \rightarrow \phi K^+ K^-$ with $\phi \rightarrow K^+ K^-$. This is the first measurement of $\eta_c \rightarrow \phi K^+ K^-$. The decay of $\eta_c \rightarrow \phi\phi$ with $\phi \rightarrow K^+ K^-$ makes up approximately 1/3 of the branching fraction of $\eta_c \rightarrow \phi K^+ K^-$.

In summary, we have observed the charmless three-body decay $B \rightarrow \phi\phi K$, which is the first example of a $b \rightarrow s\bar{s}s\bar{s}s$ transition. The branching fraction

$\mathcal{B}(B^\pm \rightarrow \phi\phi K^\pm) = (2.6^{+1.1}_{-0.9} \pm 0.3) \times 10^{-6}$ for $M_{\phi\phi} < 2.85 \text{ GeV}/c^2$, is measured with significances of 5.1σ . No signal is observed for the decay $B \rightarrow f_J(2220)K$ with $f_J(2220) \rightarrow \phi\phi$. The corresponding upper limit at 90% C.L. is $\mathcal{B}(B^\pm \rightarrow f_J(2220)K^\pm) \times \mathcal{B}(f_J(2220) \rightarrow \phi\phi) < 1.2 \times 10^{-6}$. We have also observed significant signals for $B^\pm \rightarrow \eta_c K^\pm$ with $\eta_c \rightarrow \phi\phi$, with $\eta_c \rightarrow \phi K^+ K^-$, and with $\eta_c \rightarrow 2(K^+ K^-)$, as well as a signal for $B^\pm \rightarrow J/\psi K^\pm$ with $J/\psi \rightarrow \phi K^+ K^-$. We report the first measurement of $\eta_c \rightarrow \phi K^+ K^-$ with a branching fraction of $\mathcal{B}(\eta_c \rightarrow \phi K^+ K^-) = (2.9^{+0.9}_{-0.8} \pm 1.1) \times 10^{-3}$. Our measured branching fractions for $\eta_c \rightarrow \phi\phi$ and $2(K^+ K^-)$ are smaller than those of previous experiments.

We wish to thank the KEKB accelerator group for the excellent operation of the KEKB accelerator. We acknowledge support from the Ministry of Education, Culture, Sports, Science, and Technology of Japan and the Japan Society for the Promotion of Science; the Australian Research Council and the Australian Department of Industry, Science and Resources; the National Science Foundation of China under contract No. 10175071; the Department of Science and Technology of India; the BK21 program of the Ministry of Education of Korea and the CHEP SRC program of the Korea Science and Engineering Foundation; the Polish State Committee for Scientific Research under contract No. 2P03B 01324; the Ministry of Science and Technology of the Russian Federation; the Ministry of Education, Science and Sport of the Republic of Slovenia; the National Science Council and the Ministry of Education of Taiwan; and the U.S. Department of Energy.

* on leave from Fermi National Accelerator Laboratory, Batavia, Illinois 60510

† on leave from Nova Gorica Polytechnic, Nova Gorica

[1] C.-K. Chua, W.-S. Hou, and S.-Y. Tsai, Phys. Lett. **B544**, 139 (2002).

[2] M. Hazumi (2003), hep-ph/0303089.

[3] S. Kurokawa and E. Kikutani, Nucl. Instrum. Meth. **A499**, 1 (2003).

[4] A. Abashian et al. (Belle Collaboration), Nucl. Instrum.

- Meth. **A479**, 117 (2002).
- [5] K. Hagiwara et al. (Particle Data Group), Phys. Rev. **D66**, 010001 (2002).
 - [6] R. Ammar et al. (CLEO Collaboration), Phys. Rev. Lett. **71**, 674 (1993).
 - [7] The Fox-Wolfram moment were introduced in G. C. Fox and S. Wolfram, Phys. Rev. Lett. **41**, 1581 (1978). The Fisher discriminant used by Belle is described in K. Abe *et al.*, Phys. Lett. **B517**, 309 (2001).
 - [8] H. Albrecht et al. (ARGUS Collaboration), Phys. Lett. **B241**, 278 (1990).
 - [9] J. Conrad et al., Phys. Rev. **D67**, 012002 (2003); R. D. Cousins and V. L. Highland, Nucl. Instrum. Meth. **A320**, 331 (1992); G. J. Feldman and R. D. Cousins, Phys. Rev. **D57**, 3873 (1998).
 - [10] F. Fang, T. Hojo, et al. (Belle Collaboration), Phys. Rev. Lett. **90**, 071801 (2003).